

HYDROLOGIC RESEARCH LABORATORY  
NATIONAL WEATHER SERVICE, NOAA  
HYDRO TECHNICAL NOTE - 9

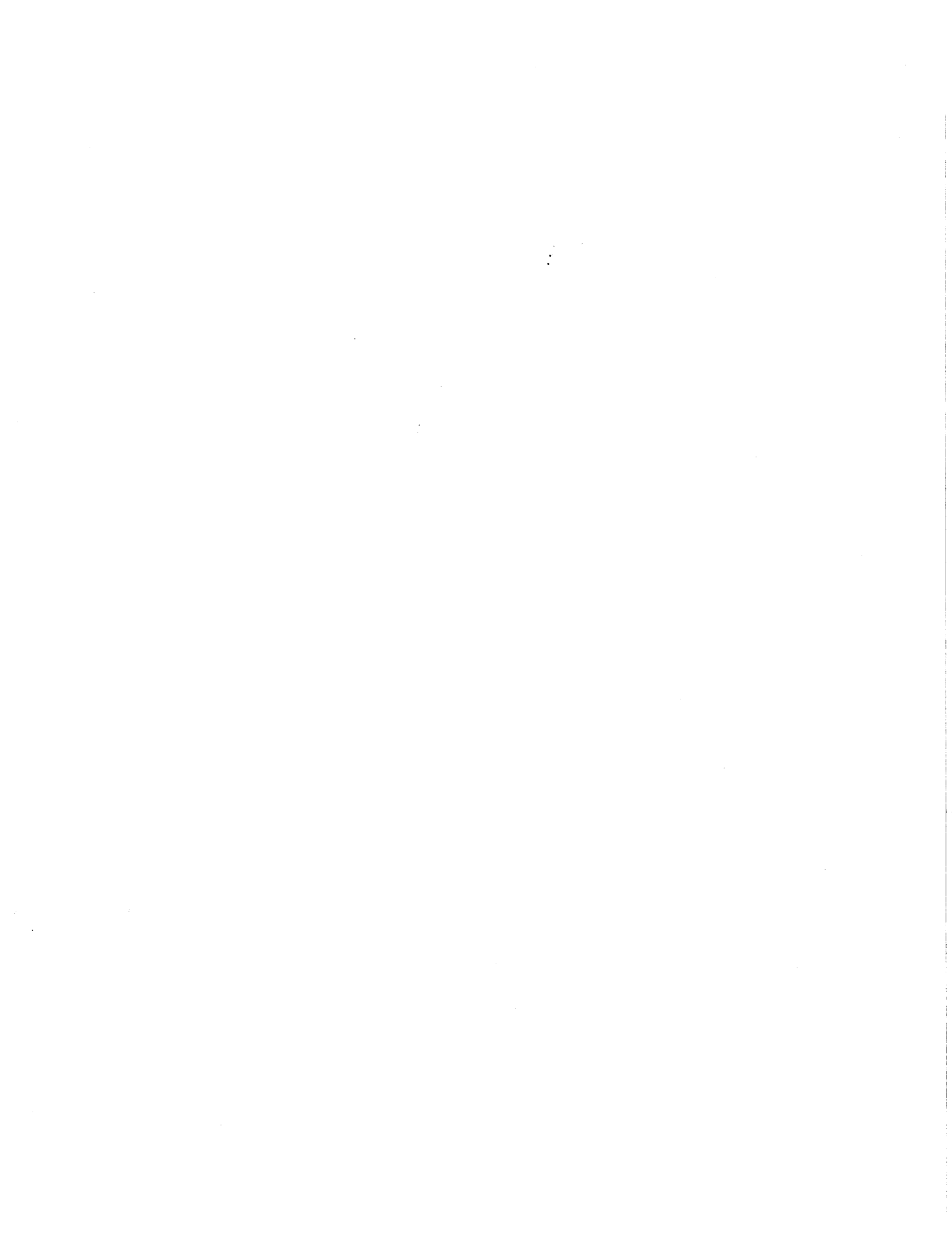
A TECHNIQUE FOR THE GENERATION OF SYNTHETIC  
RADAR-RAINFALL DATA

by

WITOLD F. KRAJEWSKI  
and  
KONSTANTINE P. GEORGAKAKOS

Hydrologic Research Laboratory  
National Weather Service  
National Oceanic and Atmospheric Administration

March 1985



## CONTENTS

	<u>Page</u>
LIST OF FIGURES.....	ii
LIST OF TABLES.....	ii
ABSTRACT.....	1
INTRODUCTION.....	1
METHOD OF GENERATION.....	2
NUMERICAL IMPLEMENTATION.....	9
SUMMARY AND CONCLUSIONS.....	18
ACKNOWLEDGEMENTS.....	18
REFERENCES.....	20
APPENDIX A: Turning Bands Method.....	A-1

FIGURES

	<u>Page</u>
Figure 1. Schematic flow chart for the generation process.....	8
Figure 2. Original daily rainfall field. GATE data for July 28, 1974.....	10
Figure 3. Generated daily radar-rainfall field. $V = 0.01$ and $\frac{1}{h} = 4$ km.....	11
Figure 4. Generated daily radar-rainfall field. $V = 0.01$ and $\frac{1}{h} = 12$ km....	12
Figure 5. Generated daily radar-rainfall field. $V = 0.01$ and $\frac{1}{h} = 20$ km....	13
Figure 6. Generated daily radar-rainfall field. $V = 0.005$ and $\frac{1}{h} = 12$ km...	14
Figure 7. $T_v$ (virtual CPU time on a PRIME/750 computer required for the generation of a rainfall field of 8250 values) as a function of the correlation distance $\frac{1}{h}$ .....	19

TABLES

Table 1. Percent errors in the generation process for nine sets of specified values.....	16
Table 2. Number of generated rainfall values that exceed 50 mm/hr.....	17

## ABSTRACT

A method of generating synthetic radar-rainfall data is described. The data are generated by imposing random noise on a given, high quality radar-rainfall field. Certain conditions are imposed on the resultant rainfall field so that the noise parameters are pre-specified. The conditions pertain to the second order statistics of the generated rainfall fields: the mean, the variance, the correlation, and the variance of the logarithmic ratio of the resultant field to the original field. Accuracy of the generation method is evaluated from implementing a test case using GARP (Global Atmospheric Research Program) Atlantic Tropical Experiment (GATE) radar data. The method can be used in a number of different, mainly hydrologic, applications. These include validation of radar and rain-gage data merging procedures, testing of various methods for computation of mean areal precipitation, and sensitivity analysis of rainfall-runoff models.

## INTRODUCTION

In recent years, radar sensors have found wide applicability in the measurement of rainfall fields. This is mainly because of their ability to map the spatial characteristics of rainfall. It is a fact, however, that in some cases, large observation errors occur [Harrold et al., 1973; Wilson and Brandes, 1979; Collier et al., 1983]. Since standard raingages offer a much more accurate way to measure point values of rainfall, procedures are being developed to merge radar and raingage observations [Brandes, 1975; Crawford, 1979; Eddy, 1979]. The purpose is to obtain the best estimate of the rainfall field, taking advantage of the spatial detail that the radar gives and of the high point accuracy of the gages.

One of the generic problems occurring during the development of merging procedures is validation. Reliable synthesis of rainfall fields can be very helpful as an alternative to costly field experiments. Using rainfall synthesis, one can control the ensemble statistics of the generated fields so that the instrument-observation errors are simulated in the validation process. Thus, it becomes possible to evaluate various merging procedures for statistically different error fields.

Because the observed rainfall fields do not exhibit ergodicity (that is, the realization statistics are not equal to the ensemble statistics), existing methods for direct generation of synthetic fields (such as those of Mejia and Rodriguez-Iturbe [1974] or Mantoglou and Wilson [1981]) are not particularly useful. These methods require the specification of the process statistics, which is infeasible for a non-ergodic process.

It is the purpose of this paper to propose a methodology that avoids the explicit specification of the rainfall field statistics by acting on the point values of the observed fields. Thus, the original field which could be, for example, a high quality radar-rainfall field, is taken as known. A random noise, which is Gaussian, isotropic, and has predefined second-order statistics, is imposed at each point of the original field. The noise level varies from point to point, based on the local original field characteristics such as magnitude and gradient.

In addition to its use in the validation of merging procedures, the proposed methodology can be used in the design of rainfall observation systems and in the testing of mean areal precipitation estimators or rainfall-runoff models, to mention only a few applications.

Other attempts to use existing high-quality radar fields for the generation of synthetic spatial rainfall were those by Greene et al. [1980]. The method presented below provides improvements over those of Greene et al. [1980], which resorted to trial and error for the specification of the statistical parameters of the noise field in order to obtain an ensemble of fields with specified spatial properties.

In the next sections, the proposed methodology is described, followed by a discussion of an example implementation.

#### METHOD OF GENERATION

The basic idea of the procedure is to generate fields from an existing high quality radar field by imposing a noise field of known statistics such that the ensemble of the resultant realizations meets certain conditions. The conditions pertain to the spatially-averaged second order statistics of the generated fields.

It is due to the imposed conditions that the second order statistics of the noise field are obtained. Such a procedure was made necessary by the lack of knowledge of the radar-noise field statistics.

If  $G(x,y)$  is the generated field and  $O(x,y)$  is the original, high-quality radar field, then the error field  $\Delta(x,y)$  is commonly [Hudlow et al., 1979] expressed as:

$$\Delta(x,y) = \log_{10} \left( \frac{G(x,y)}{O(x,y)} \right) \quad (x,y) \in A \quad (1)$$

where  $x,y$  are the field-point coordinates, and  $A$  is the field domain.

For the purposes of this study we take  $\Delta(x,y)$  to be the product of a random field and a deterministic component according to:

$$\Delta(x,y) = \epsilon(x,y) \cdot S(x,y) \quad (2)$$

In Eq. (2),  $\epsilon(x,y)$  is a stationary and, in general, anisotropic, Gaussian random field of mean  $\mu$ , variance  $\sigma^2$ , and correlation function  $\rho(\tau_1, \tau_2)$  with  $\tau_1, \tau_2$  denoting spatial lags in the two directions  $x$  and  $y$ .  $S(x,y)$  is a deterministic function which makes  $\Delta(x,y)$  a nonstationary random field. We adopt the form of  $S(x,y)$  given by Greene et al. [1980]:

$$S(x,y) = \frac{|\overline{\nabla O(x,y)}| \cdot O_{\max}(x,y) + O(x,y) \cdot |\overline{\nabla O(x,y)}|_{\max}}{2 |\overline{\nabla O(x,y)}|_{\max} \cdot O_{\max}(x,y)} \quad (3)$$

where:

$|\overline{\nabla O(x,y)}|$  is the average absolute value of the gradient computed in four directions around the point  $(x,y)$  in the original field,

$|\overline{\nabla O(x,y)}|_{\max}$  is the maximum absolute value of the gradient in the original field,

$O(x,y)$  is the original field value at the point  $(x,y)$ , and

$O_{\max}(x,y)$  is the maximum value in the original field.

The form of function  $S(x,y)$  in Eqs. (3) and (2) implies high errors where high gradients and high magnitudes occur.

We note at this point that the development of the methodology is independent of the particular form of  $S(x,y)$  in Eq. (3), so that any deterministic, real function of  $(x,y)$  can be used.

Eliminating  $\Delta(x,y)$  from Eqs. (1) and (2) yields

$$G(x,y) = O(x,y) \cdot 10^{\varepsilon(x,y)} \cdot S(x,y) \quad (4)$$

If one has a mechanism for generating the random component field  $\varepsilon(x,y)$ , then, using Eq. (4) and the original high-quality radar field  $O(x,y)$ , one can produce a realization of  $G(x,y)$ .

It should be noted here, that the use of Eq. (4) for the generation of  $G(x,y)$  leaves the zero-rainfall areas of  $O(x,y)$  unaltered. The changes in the non-zero areas of  $O(x,y)$  are the ones that produce fields with the desirable statistics.

There are several methods for the generation of  $\varepsilon(x,y)$ , given its statistical parameters  $\mu$ ,  $\sigma^2$ , and  $\rho(\tau_1, \tau_2)$ . The Turning Bands Method (TBM) presented by Mantoglou and Wilson [1982] is an efficient one in terms of accuracy and cost. A short description of the TBM is given in the Appendix.

The TBM gives us a way to generate the field  $\varepsilon(x,y)$  in Eq. (4) if its second order statistics are known. We obtain these statistics by imposing certain conditions on the generated fields.

Because  $G(x,y)$  is a nonstationary random field, we need to specify operational measures of its statistical properties. Thus, we define:

- 1) The spatial mean  $R$  of the field as:

$$R = \frac{1}{|A|} \int_A E\{G(x,y)\} dx dy \quad (5)$$

where  $A$  is the generation domain with area  $|A|$ , and  $E\{\cdot\}$  denotes the expectation of the value of  $G$  at the point  $(x,y)$ .

2) The spatially-averaged variance P of the field G(x,y) as:

$$P = \frac{1}{|A|} \int_A E\{[G(x,y) - E\{G(x,y)\}]^2\} dx dy \quad (6)$$

3) The spatially-averaged correlation  $\rho_x(\tau_1)$  of the field G(x,y) in direction x as:

$$\rho_x(\tau_1) = \frac{1}{|A|} \int_A \frac{E\{[G(x,y) - E\{G(x,y)\}] \cdot [G(x+\tau_1,y) - E\{G(x+\tau_1,y)\}]\}}{\sqrt{E\{[G(x,y) - E\{G(x,y)\}]^2\}} \sqrt{E\{[G(x+\tau_1,y) - E\{G(x+\tau_1,y)\}]^2\}}} dx dy \quad (7)$$

with  $\tau_1$  denoting the spatial lag in the x-direction.

Similarly, the correlation  $\rho_y(\tau_2)$  in direction y is defined as:

$$\rho_y(\tau_2) = \frac{1}{|A|} \int_A \frac{E\{[G(x,y) - E\{G(x,y)\}] \cdot [G(x,y+\tau_2) - E\{G(x,y+\tau_2)\}]\}}{\sqrt{E\{[G(x,y) - E\{G(x,y)\}]^2\}} \sqrt{E\{[G(x,y+\tau_2) - E\{G(x,y+\tau_2)\}]^2\}}} dx dy \quad (8)$$

with  $\tau_2$  denoting the spatial lag in the y-direction.

Equations (5), (6), (7), and (8) describe the spatially averaged field-expected value, field-variance and field-correlation of G(x,y).

Another measure of variance used often in the radar literature [Hudlow, 1979] in place of Eq. (6) is the variance V of the logarithmic ratio of Eq. (1), defined as:

$$V = \frac{1}{|A|} \int_A E\{\log_{10}^2\left(\frac{G(x,y)}{O(x,y)}\right)\} dx dy - \frac{1}{|A|} \int_A E^2\{\log_{10}\left(\frac{G(x,y)}{O(x,y)}\right)\} dx dy \quad (9)$$

By setting the expressions in Eqs. (5), (6) or (9), (7), and (8) to prespecified values, one can, in principle, obtain expressions for  $\mu$ ,  $\sigma^2$ , and  $\rho(\tau_1, \tau_2)$ . Then, one can generate the  $\varepsilon(x,y)$  field using the TBM and subsequently generate the G(x,y) field from (4).

The first step would be to obtain expressions for the expectations:

$$E_1 = E\{G(x,y)\}$$

$$E_2 = E\{[G(x,y) - E_1]^2\}$$

$$E_3 = \frac{E\{[G(x,y) - E_1] \cdot [G(x+\tau_1,y) - E\{G(x+\tau_1,y)\}]\}}{\sqrt{E\{[G(x,y) - E_1]^2\}} \sqrt{E\{[G(x+\tau_1,y) - E\{G(x+\tau_1,y)\}]^2\}}}$$

$$E_4 = \frac{E\{[G(x,y) - E_1] \cdot [G(x,y+\tau_2) - E\{G(x,y+\tau_2)\}]\}}{\sqrt{E\{[G(x,y) - E_1]^2\}} \sqrt{E\{[G(x,y+\tau_2) - E\{G(x,y+\tau_2)\}]^2\}}}$$

$$E_5 = E\{\log_{10}\left(\frac{G(x,y)}{O(x,y)}\right)\}$$

and

$$E_6 = E\{\log_{10}^2\left(\frac{G(x,y)}{O(x,y)}\right)\}$$

Because of (4), we start from the relationships [Vanmarcke, 1983]:

$$Y = e^Z \quad (10)$$

$$E\{Y\} = \exp\left\{\frac{1}{2} \cdot \sigma_Z^2 + \mu_Z\right\} \quad (11)$$

$$E\{[Y - E\{Y\}]^2\} = \exp\{2\sigma_Z^2 + 2\mu_Z\} - \exp\{\sigma_Z^2 + 2\mu_Z\} \quad (12)$$

and

$$\rho_Y(\tau_1, \tau_2) = \frac{\exp\{\sigma_Z^2 \cdot \rho_Z(\tau_1, \tau_2)\} - 1}{\exp\{\sigma_Z^2\} - 1} \quad (13)$$

where  $\exp\{\cdot\}$  denotes exponentiation and  $Z$  is a Gaussian, stationary, anisotropic, random field with mean  $\mu_Z$ , standard deviation  $\sigma_Z$ , and correlation coefficient  $\rho_Z(\tau_1, \tau_2)$  for lags  $\tau_1$  and  $\tau_2$ .

Eqs. (10) through (13) also hold true for the random variables  $Z$  and  $Y$  [Vanmarcke, 1983]. Therefore, one can use them in the case of nonstationary and anisotropic random fields by applying them at each point  $(x,y)$  in the field for the random variables  $Z(x,y)$  and  $Y(x,y)$  connected by Eq. (10). Thus, Eqs. (4) and (10) through (13) can be used to derive expressions for the expectations  $E_1$  and  $E_2$ :

$$E_1 = O(x,y) \cdot \exp\left\{\frac{1}{2} (\ln 10)^2 \cdot S^2(x,y) \cdot \sigma^2 + (\ln 10) \cdot S(x,y) \cdot \mu\right\} \quad (14)$$

$$E_2 = O^2(x,y) \cdot [\exp\{2(\ln 10)^2 \cdot S^2(x,y) \cdot \sigma^2 + 2(\ln 10) \cdot S(x,y) \cdot \mu\} - \exp\{(\ln 10)^2 \cdot S^2(x,y) \cdot \sigma^2 + 2(\ln 10) \cdot S(x,y) \cdot \mu\}] \quad (15)$$

For  $S(x,y)$  reasonably smooth in the generation domain A and for small values of  $\tau_1$  and  $\tau_2$ , one can use Eq. (13), which is strictly true for stationary fields, to derive approximate expressions for  $E_3$  and  $E_4$ :

$$E_3 = \frac{\exp\{(\ln 10)^2 \cdot S^2(x,y) \cdot \sigma^2 \cdot \rho(\tau_1, 0)\} - 1}{\exp\{(\ln 10)^2 \cdot S^2(x,y) \cdot \sigma^2\} - 1} \quad (16)$$

$$E_4 = \frac{\exp\{(\ln 10)^2 \cdot S^2(x,y) \cdot \sigma^2 \cdot \rho(0, \tau_2)\} - 1}{\exp\{(\ln 10)^2 \cdot S^2(x,y) \cdot \sigma^2\} - 1} \quad (17)$$

The expectations  $E_5$  and  $E_6$  are (see Eq. (2)):

$$E_5 = S(x,y) \cdot \mu \quad (18)$$

$$E_6 = S^2(x,y) \cdot (\sigma^2 + \mu^2) \quad (19)$$

If one specifies design values for  $R$ ,  $V$  or  $P$ ,  $\rho_x(\tau_1)$ , and  $\rho_y(\tau_2)$ , in Eqs. (5), (9) or (6), (7), and (8), respectively, and uses the expressions in Eqs. (14) through (19), one obtains the set of equations:

$$\frac{1}{|A|} \int_A O(x,y) \cdot \exp\left\{\frac{1}{2} (\ln 10)^2 \cdot S^2(x,y) \cdot \sigma^2 + (\ln 10) \cdot S(x,y) \cdot \mu\right\} dx dy = R_0 \quad (20)$$

$$\frac{\sigma^2}{|A|} \int_A S^2(x,y) dx dy = V_0 \quad (21)$$

$$\frac{1}{|A|} \int_A O^2(x,y) \cdot [\exp\{2(\ln 10)^2 \cdot S^2(x,y) \cdot \sigma^2 + 2(\ln 10) \cdot S(x,y) \cdot \mu\} - \exp\{(\ln 10)^2 \cdot S^2(x,y) \cdot \sigma^2 + 2(\ln 10) \cdot S(x,y) \cdot \mu\}] dx dy = P_0 \quad (22)$$

$$\frac{1}{|A|} \int_A \frac{\exp\{(\ln 10)^2 \cdot S^2(x,y) \cdot \sigma^2 \cdot \rho(\tau_1, 0)\} - 1}{\exp\{(\ln 10)^2 \cdot S^2(x,y) \cdot \sigma^2\} - 1} dx dy = \rho_{x_0}(\tau_1) \quad (23)$$

and

$$\frac{1}{|A|} \int_A \frac{\exp\{(\ln 10)^2 \cdot S^2(x,y) \cdot \sigma^2 \cdot \rho(0,\tau_2)\} - 1}{\exp\{(\ln 10)^2 \cdot S^2(x,y) \cdot \sigma^2\} - 1} dx dy = \rho_{y_0}(\tau_2) \quad (24)$$

where  $R_0$ ,  $V_0$ ,  $P_0$ ,  $\rho_{x_0}(\tau_1)$ ,  $\rho_{y_0}(\tau_2)$  are design values. Solving simultaneously the equations (20), (21) or (22), (23), and (24), one can obtain values for  $\mu$ ,  $\sigma^2$ ,  $\rho(\tau_1, 0)$ , and  $\rho(0, \tau_2)$ .

Assuming an exponential correlation function for  $\varepsilon(x,y)$ , of the type

$$\rho(\tau_1, \tau_2) = \exp\{-(h_1^2 \cdot \tau_1^2 + h_2^2 \cdot \tau_2^2)^{1/2}\}, \quad (25)$$

knowledge of  $\rho(\tau_1, 0)$  and  $\rho(0, \tau_2)$  gives estimates of  $h_1$ ,  $h_2$ . Therefore,  $\rho(\tau_1, \tau_2)$  can be defined.

With  $\mu$ ,  $\sigma^2$ , and  $\rho(\tau_1, \tau_2)$  known, one can use the TBM to generate realizations of  $\varepsilon(x,y)$ .

In the particular case of an isotropic  $\varepsilon(x,y)$  field with correlation function

$$\rho(\tau) = \exp[-h \cdot \tau], \quad (26)$$

the design equations (23) and (24) consolidate to the following:

$$\frac{1}{|A|} \int_A \frac{\exp\{(\ln 10)^2 \cdot S^2(x,y) \cdot \sigma^2 \cdot \rho(\tau)\} - 1}{\exp\{(\ln 10)^2 \cdot S^2(x,y) \cdot \sigma^2\} - 1} dx dy = \rho_{G_0}(\tau) \quad (27)$$

where  $\rho_{G_0}(\tau)$  is the design value of the correlation for the  $G(x,y)$  field.

Figure 1 shows a schematic flowchart of the generation process: The next section presents an example of application of the proposed methodology.

STEP 1: ORIGINAL RADAR FIELD:  $O(x,y)$

STEP 2: COMPUTE DETERMINISTIC COMPONENT:  $S(x,y)$   
- Eq. (3)

STEP 3: SPECIFY DESIGN VALUES:  $R_0, P_0$  or  $V_0, \rho_{x_0}(\tau_1), \rho_{y_0}(\tau_2)$

STEP 4: COMPUTE  $\mu, \sigma, \rho(\tau_1, \tau_2)$   
- Eqs. (20), (21) or (22), (23), (24), (25)

STEP 5: GENERATE ONE REALIZATION OF THE NOISE FIELD  $\epsilon(x,y)$  USING THE TBM  
- APPENDIX

STEP 6: GENERATE A RAINFALL FIELD:  $G(x,y)$   
- Eq. (4)

STEP 7: MORE FIELDS?  
IF YES -- GO TO STEP 5  
IF NO -- STOP

Figure 1. Schematic flowchart for the generation process.

## NUMERICAL IMPLEMENTATION

This section presents an example of the generation of rainfall fields from an original, high-quality radar field. Accuracy of preservation of the design-statistics in the generated ensemble of rainfall fields is studied in connection with the number of generated fields and the magnitude of the statistics themselves.

The original field consisted of daily radar data from the international GARP Atlantic Tropical Experiment (GATE) conducted in 1974. A detailed description of the GATE data is given by Hudlow and Patterson [1979]. The original radar field (Figure 2) corresponds to spatially averaged daily accumulations for July 28, 1974. Spatial averages were computed in 4 km by 4 km domains.

For the purposes of this example, the design equations (20), (21), (22), and (27) were studied.

The number of lines  $L$  and the number of harmonics  $M$  of the TBM generator took the values 16 and 100 respectively. Other parameters were specified as a function of the inverse correlation distance  $h$  (Eq. 26). Based on the suggestions by Mantoglou and Wilson [1981], the maximum frequency  $\Omega$  was set equal to  $40 \cdot h$ . The chosen set of parameters ensures accurate performance of the TBM.

During the example runs, we generated rainfall fields from the original radar field with mean equal to the spatial average of the original field (1.16 mm/hr), and with prespecified values for the logarithmic-ratio variance  $V_0$  (0.005, 0.01, 0.03). The correlation condition consisted of specifying values for the correlation distance  $1/h$  of the  $\varepsilon(x,y)$  field (4 km, 12 km, 20 km).

For illustration purposes Figures 3, 4, 5, and 6 present examples of generated fields with various second-order statistics based on the high-quality radar field of Figure 2. In Figures 3, 4, and 5,  $V$  was set equal to 0.01 and  $1/h$  took the values 20 km, 12 km, and 4 km respectively. Figure 6 had  $V=0.005$  and  $1/h = 12$  km. In all figures dashed lines correspond to contours at the 1.5mm/hr level, solid lines correspond to contours at the 4 mm/hr level, and thick solid lines correspond to contours at the 11.5 mm/hr level.

In a true generation process, one specifies the value of the correlation of the  $G(x,y)$  field and then, using Eq. (27), one obtains the value of the correlation of the  $\varepsilon(x,y)$  field. Since our purpose was to study the capabilities of the method for a range of correlation values, we specified several values of the correlation of  $\varepsilon(x,y)$  by specifying the correlation distance  $1/h$  and then we used Eq. (27) to compute the correlation  $\rho_G$  of the  $G(x,y)$  field. Given that Eqs. (23), (24), and, consequently, Eq. (27) are strictly true for stationary fields  $S(x,y) = \varepsilon(x,y)$ , we computed  $\rho_G$  for the smallest possible lag  $\tau = 4$  km so that  $S(x,y) = S(x+\tau,y) = S(x,y+\tau)$ .

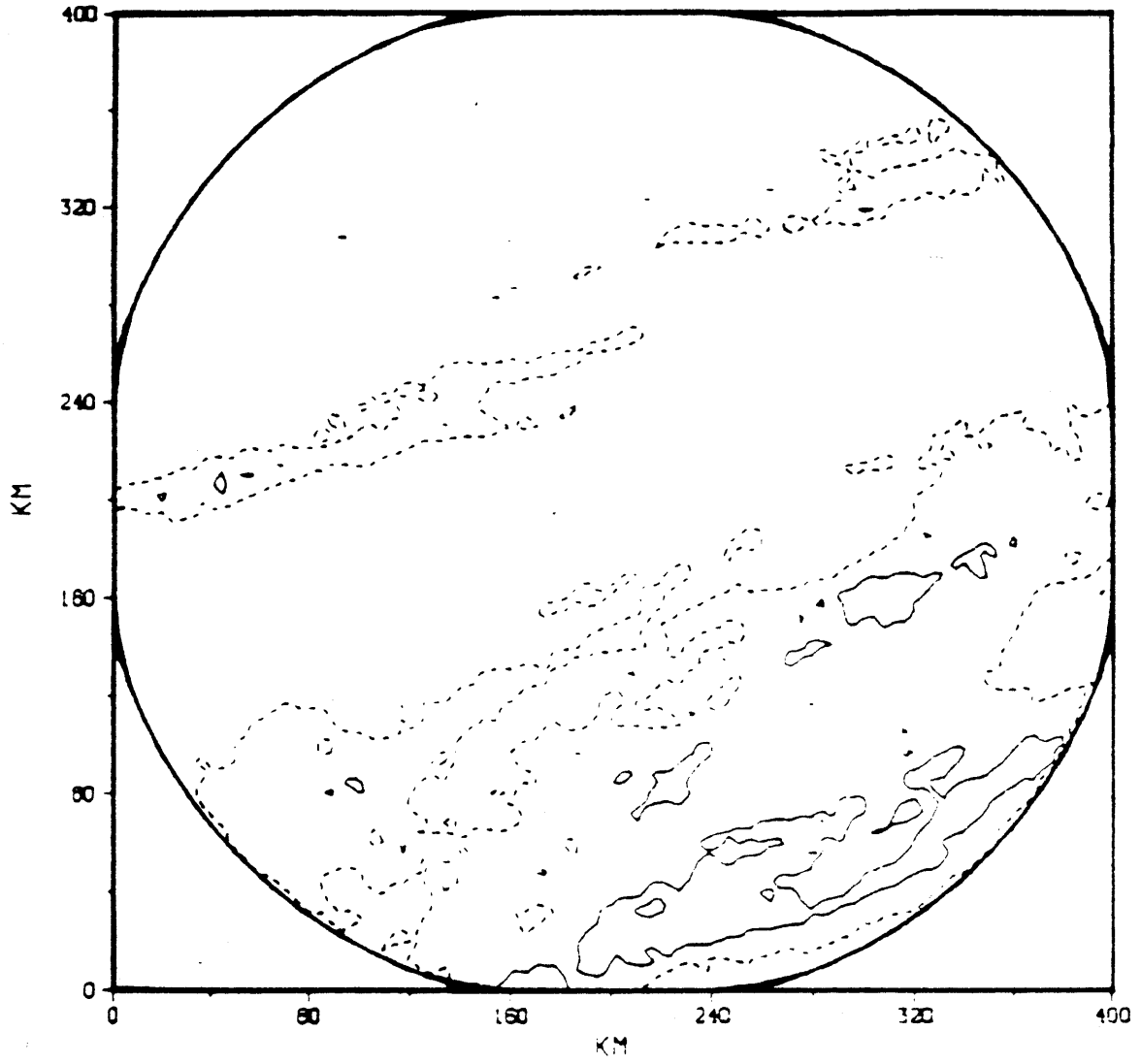


Figure 2. Original daily rainfall field. GATE data for July 28, 1974.

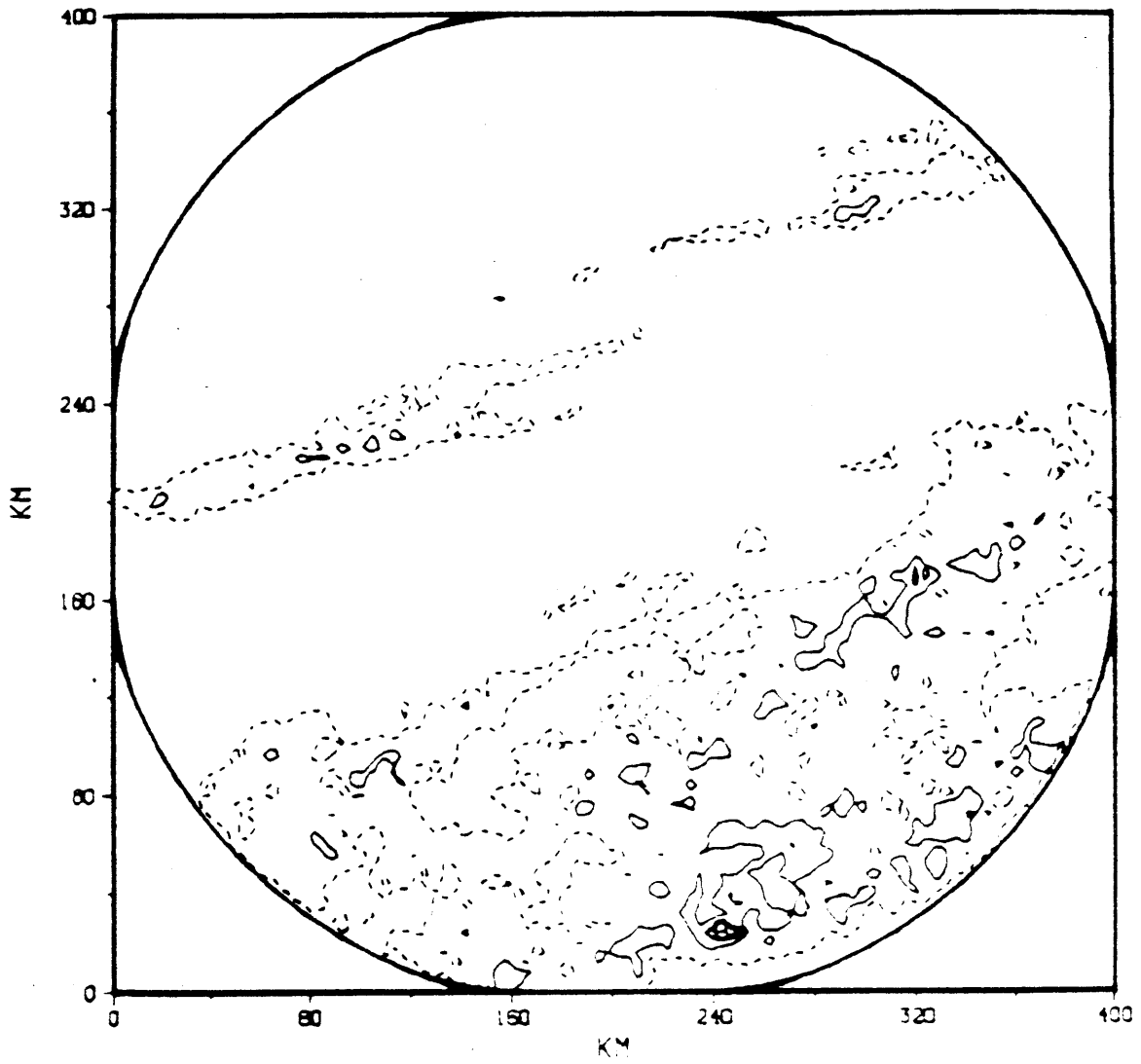


Figure 3. Generated daily radar-rainfall field.  $V = 0.01$  and  $1/h = 4$  km.

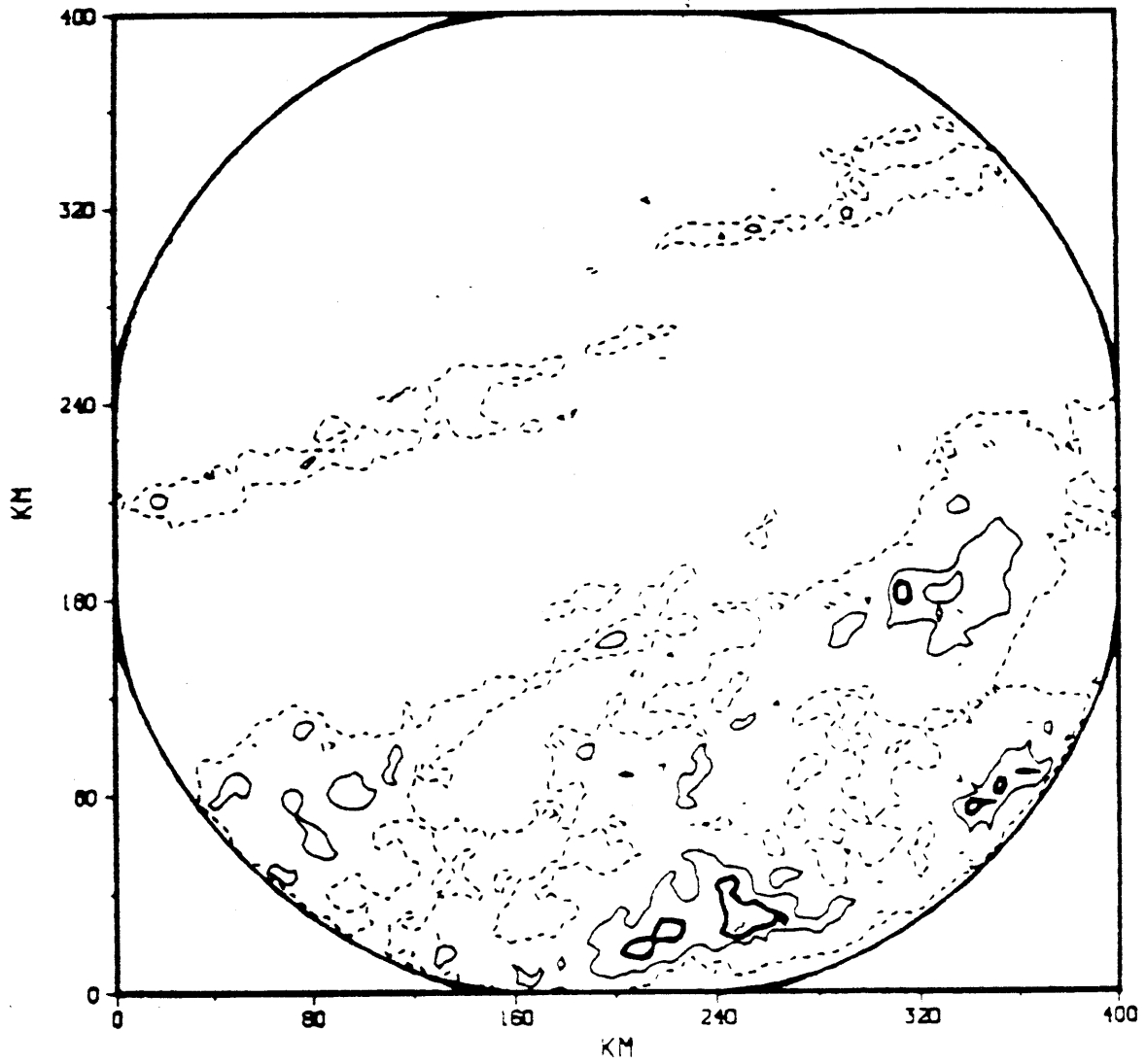


Figure 4. Generated daily radar-rainfall field.  $V = 0.01$  and  $1/h = 12$  km.

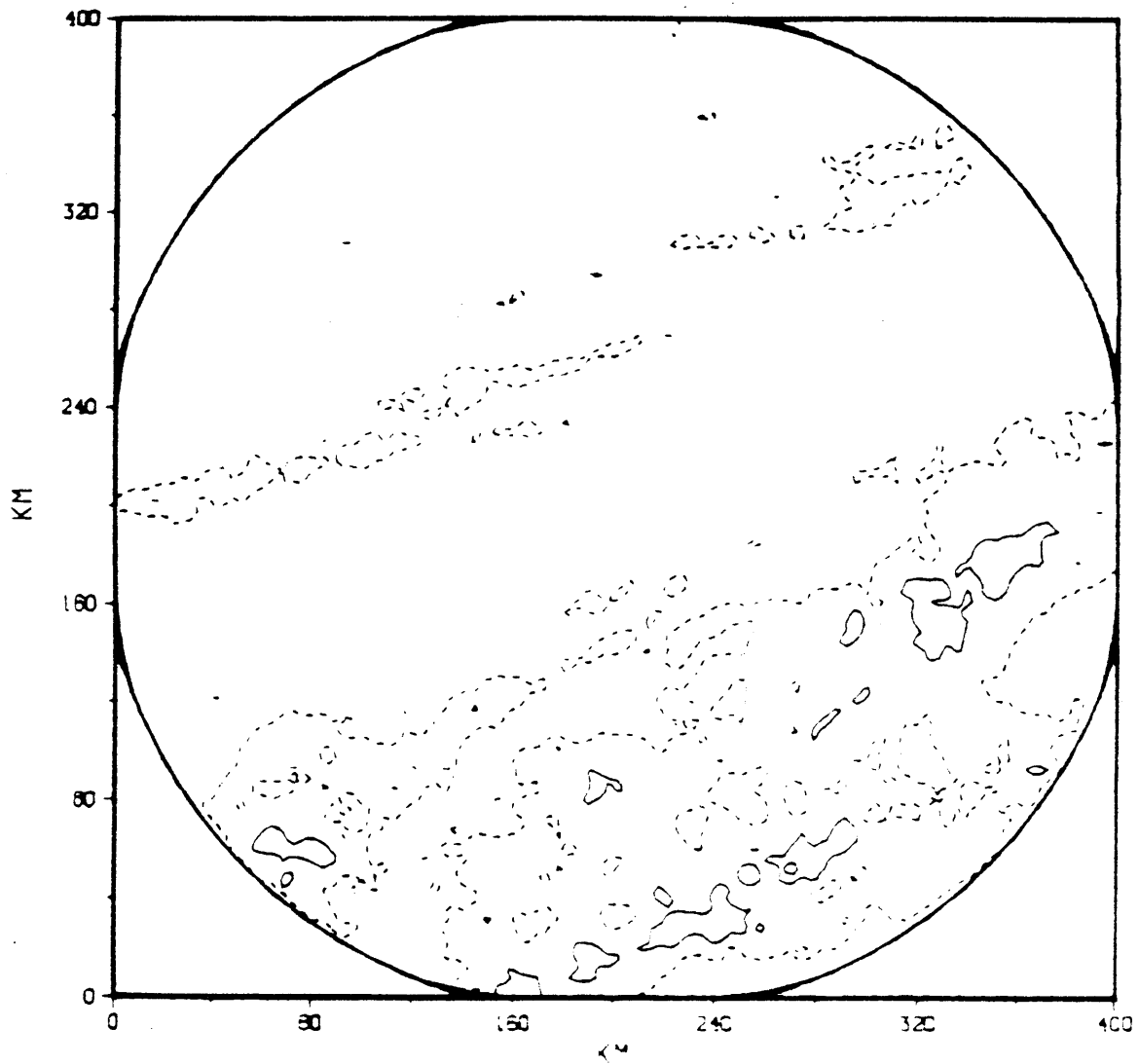


Figure 5. Generated daily radar-rainfall field.  $V = 0.01$  and  $1/h = 20$  km.

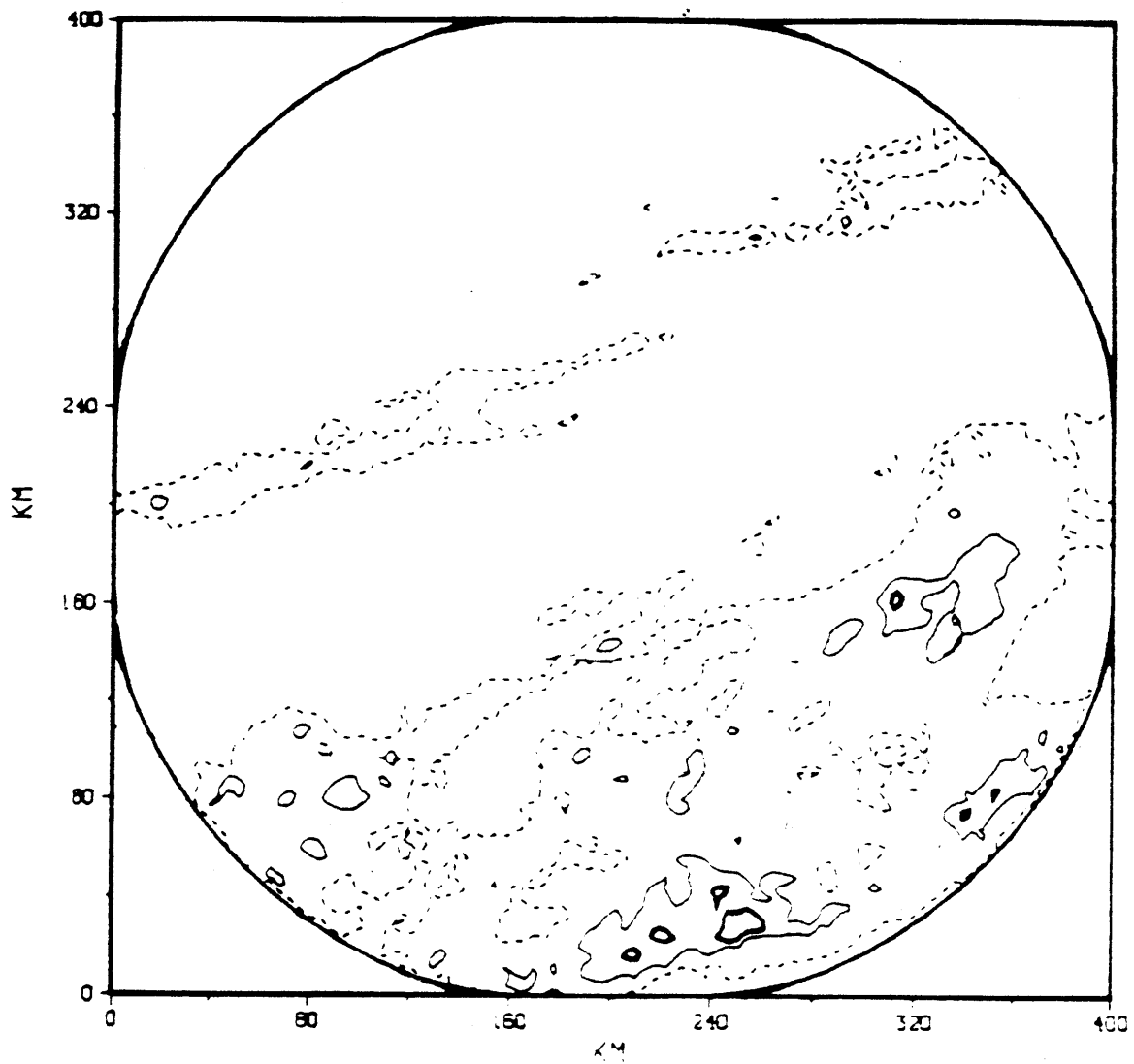


Figure 6. Generated daily radar-rainfall field.  $V = 0.005$  and  $1/h = 12$  km.

For all the combinations of  $R_0$ ,  $V_0$ , and  $1/h$ , we generated three ensembles of rainfall fields, with the number of fields per ensemble, NS, equal to 10, 25, and 50. We then computed the statistics  $R$ ,  $V$ ,  $P$ ,  $\rho_G(\tau=4 \text{ km})$  for each ensemble and we compared them with their theoretical values obtained from Eqs. (20), (21), (22), and (27), respectively. We also computed  $\mu$  and  $\sigma^2$  from each ensemble and compared them to the values obtained by solving Eqs. (20) and (21). Thus, we were able to evaluate the accuracy of the TBM generator.

Because the specification of high  $V$  and  $P$  statistics will sometimes yield physically unacceptable values of the precipitation rates, we monitored the number of values exceeding an arbitrarily chosen rate, set to 50 mm/hr, which is close to the observed world record value of 55 mm/hr for daily data [Chow, 1964]. Consequently, we give guidelines on the specification of  $V$ , which is a normalized measure, so that generation of realistic rainfall fields results.

Table 1 contains the results obtained for all cases. The results form nine sets that cover the nine combinations of  $V$  and  $1/h$  values specified. In Table 1, the sets are arranged in three rows and three columns. Each row has the value of  $V$  fixed, while each column has the value of  $1/h$  fixed as shown below to:

Row 1: $V = 0.005$	Column 1: $\frac{1}{h} = 4 \text{ km}$
Row 2: $V = 0.01$	Column 2: $\frac{1}{h} = 12 \text{ km}$
Row 3: $V = 0.03$	Column 3: $\frac{1}{h} = 20 \text{ km}$

For all cases, the value of  $R$  remained equal to 1.16 mm/hr.

The table displays the prespecified values of  $\mu$ ,  $\sigma^2$ ,  $V$ ,  $P$ ,  $\rho_G(\tau=4 \text{ km})$ , as well as the percent errors  $\frac{(\text{Prespecified Value}) - (\text{Computed Value})}{(\text{Prespecified Value})} \cdot 100$ , that were realized during the generation process. The field mean  $R$ , not included in the table, had an error of less than one percent for all of the cases.

Inspection of the prespecified  $P$  values of Table 1 reveals that a wide range of G-field variances was included, ranging from 0.73 mm<sup>2</sup>/hr<sup>2</sup> up to 4.51 mm<sup>2</sup>/hr<sup>2</sup>. Similarly, the prespecified  $\rho_G$  values suggest that a wide range of G-field correlations was studied: from 0.32 up to 0.72.

The values of the percent errors in Table 1, excluding the ones corresponding to  $P$  for sets 7, 8, and 9, are all less than 16% and, in most cases, less than 10%. In general, better accuracy is obtained as NS increases, but accuracy is very good even with NS=10.

The results corresponding to statistic  $P$ , for  $V$  specified equal to 0.03 (last row of sets), show abnormal behavior compared to the rest of the results in the same row of sets and for all the rest of the variables. The cause of this phenomenon is the nonlinear relationship between  $V$  and  $P$  (see Eqs. (6) and (9)). Because there is an exponential relationship between  $V$  and  $P$  (one cannot prespecify both  $V$  and  $P$ ), small errors in approximating the specified value of  $V$  can (depending on the form of  $S(x,y)$ ) lead to pronounced errors in the preservation of  $P$ , when  $V$  and  $P$  have high specified values. At any rate, the number of unrealistic precipitation values which resulted from the generation process, for  $V$  specified at 0.03, was unacceptable (see Table 2).

Table 1. Percent errors in the generation process for nine sets of specified values

Statistic	Set 1			Set 2			Set 3					
	Specified	NS=10	NS=25	NS=50	Specified	NS=10	NS=25	NS=50	Specified	NS=10	NS=25	NS=50
$\mu$	-.08	0.0	0.0	0.0	-.08	-12.5	0.0	0.0	-.08	-12.5	12.5	12.5
$\sigma^2$	.24	12.5	8.3	4.2	.24	12.5	8.3	4.0	.24	12.5	8.3	4.0
V	.005	12.0	6.0	4.0	.005	6.0	4.0	2.0	.005	14.0	8.0	2.0
P(mm <sup>2</sup> /hr <sup>2</sup> )	.73	8.2	2.7	0.0	.73	0.0	-2.7	-4.0	.73	11.0	6.8	2.7
$\rho_G(\tau=4 \text{ km})$	.32	-12.5	-15.6	-15.6	.63	-12.9	-14.5	-14.5	.72	-9.7	-11.1	-11.1

Statistic	Set 4			Set 5			Set 6					
	Specified	NS=10	NS=25	NS=50	Specified	NS=10	NS=25	NS=50	Specified	NS=10	NS=25	NS=50
$\mu$	-.16	0.0	0.0	0.0	-.16	-6.3	0.0	0.0	-.16	-6.3	12.5	12.5
$\sigma^2$	.47	12.8	6.4	4.3	.47	10.6	4.3	2.1	.47	10.6	6.4	4.3
V	.01	13.0	7.0	4.0	.01	7.0	4.0	2.0	.01	14.0	9.0	3.0
P(mm <sup>2</sup> /hr <sup>2</sup> )	1.16	4.3	0.0	-2.6	1.16	-2.6	-14.7	-10.3	1.16	14.7	11.2	4.3
$\rho_G(\tau=4 \text{ km})$	.32	-9.4	-15.6	-15.6	.63	-12.9	-12.9	-12.9	.72	-9.7	-11.1	-11.1

Statistic	Set 7			Set 8			Set 9					
	Specified	NS=10	NS=25	NS=50	Specified	NS=10	NS=25	NS=50	Specified	NS=10	NS=25	NS=50
$\mu$	-.50	0.0	0.0	-2.0	-.50	-2.0	0.0	0.0	-.50	-4.0	6.0	6.0
$\sigma^2$	1.42	12.0	6.4	4.3	1.42	10.6	5.6	3.5	1.42	12.0	7.7	4.2
V	.03	12.7	7.0	3.7	.03	7.0	4.0	1.7	.03	13.7	9.0	3.0
P(mm <sup>2</sup> /hr <sup>2</sup> )	4.51	55.0	46.1	38.6	4.51	49.7	42.6	37.5	4.51	51.2	48.6	39.5
$\rho_G(\tau=4 \text{ km})$	.32	12.9	-9.4	-12.5	.63	-11.3	-11.3	-12.9	.72	-9.7	-9.7	-9.7

Table 2. Number of generated rainfall values that exceed 50 mm/hr.

1/h (km)	NS=10			NS=25			NS=50		
	4	12	20	4	12	20	4	12	20
$V_0$									
0.005	1	1	0	3	2	0	5	4	1
0.010	1	1	0	11	7	3	27	21	15
0.030	32	41	36	92	113	99	193	232	219

Therefore, the third row of sets will not normally be used in a true generation of realistic precipitation fields.

The virtual CPU time required for generation depends mainly on the correlation distance  $1/h$  specified for the  $\epsilon(x,y)$  field. The time-consuming TBM generator used more time to generate a weakly correlated field than to generate a strongly correlated one. The CPU time required to generate one field on a PRIME/750 computer PRIMOS operating system is given in minutes in Figure 7, as a function of the correlation distance  $1/h$ . Note that a total of over 8000 values were generated in each rainfall field.

#### SUMMARY AND CONCLUSIONS

A method for generation of radar precipitation fields was described. The method works by imposing a noise field on high quality radar rainfall fields. The noise parameters are determined based on a set of conditions pertaining to the resultant field. In that way, non-stationary, non-ergodic fields can be simulated.

Since the original and the 'observation' (original + noise) fields are known, the method can be used in the validation procedures of various hydrologic models (radar and rain-gage data merging, mean areal precipitation estimation, rainfall-runoff). The example given shows that the accuracy of the preservation of the required statistics is very good, especially for realistic values of the variance measure ( $V < 0.01$ ), even for a relatively small number of realizations ( $NS \leq 25$ ). The method proposed is flexible in that one can generate fields with a wide range of second-order statistics from one high-quality radar field.

When the technique is used to investigate radar and rain-gage data merging, a procedure is required to synthesize the gage data. The authors are investigating techniques to generate gage values in work under preparation.

#### ACKNOWLEDGEMENTS

The work was performed under the National Research Council and National Oceanic and Atmospheric Administration sponsorship, while both authors were NRC-NOAA Research Associates. The comments of Michael D. Hudlow and Edward R. Johnson of the Hydrologic Research Laboratory of the National Weather Service (HRL/NWS), James A. Smith of the Interstate Commission for the Potomac River Basin, Aristotelis Mantoglou of MIT, and Lianne T. Iseley of HRL/NWS are gratefully acknowledged.

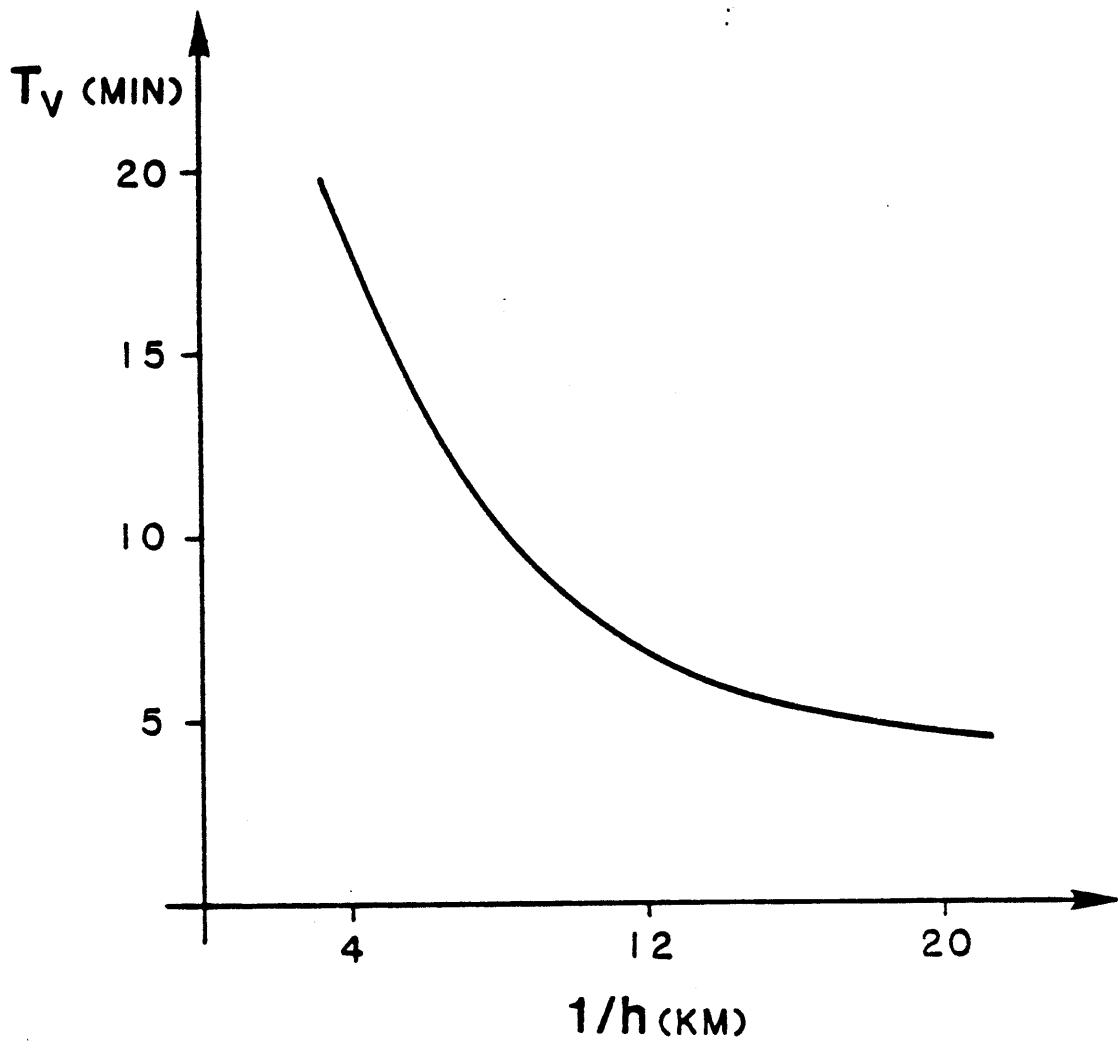


Figure 7.  $T_V$  (virtual CPU time on a PRIME/750 computer required for the generation of a rainfall field of 8250 values) as a function of the correlation distance  $1/h$ .

## REFERENCES

- Brandes, E.A., Optimizing rainfall estimates with the aid of radar, Journal of Applied Meteorology, 14, 1339-1345, 1975.
- Chow, V.T. (Editor-in-Chief), Handbook of Applied Hydrology, McGraw-Hill, 9-47, 1964.
- Collier, C.G., P.R. Larke, and B.R. May, A weather radar correction procedure for real-time estimation of surface rainfall, Quart. J. R. Met. Soc., 109, 589-608, 1983.
- Crawford, K.C., Considerations for the design of a hydrologic data network using multivariate sensors, Water Resources Research, 15(6), 1752-1762, 1979.
- Eddy, A., Objective analysis of convective scale rainfall using gages and radar, Journal of Hydrology, 44, 125-134, 1979.
- Greene, D.R., M.D. Hudlow, and E.R. Johnson, A test of some objective analysis procedures for merging radar and rain-gage data, Preprints of the 19th Conference on Radar Meteorology, American Meteorological Society, Miami, Florida, 470-479, April 1980.
- Harrold, T.W., E.J. English, and C.A. Nicholas, The Dee weather radar project: the measurement of area precipitation using radar, Weather, 28, 332-338, 1973.
- Hudlow, M.D., R. Arkell, V. Patterson, P. Pytlowany, and F. Richards, Calibration and Intercomparison of the GATE C-Band Radars, NOAA Technical Report EDIS 31, U.S. Department of Commerce, Washington, D.C., pp. 98, 1979.
- Hudlow, M.D. and V.L. Patterson, GATE Radar Rainfall Atlas, NOAA Special Report, U.S. Department of Commerce, Washington, D.C., pp. 155, 1979.
- Mantoglou, A. and J.L. Wilson, Simulation of Random Fields with the Turning Bands Method, Report No. 264, Ralph M. Parsons Laboratory, Hydrology and Water Resources Systems, Department of Civil Engineering, MIT, 1981.
- Mantoglou, A. and J.L. Wilson, The Turning Bands Method for simulation of random fields using line generation by a spectral method, Water Resources Research, 18(5), 1379-1394, 1982.
- Mejia, J. and I. Rodriguez-Iturbe, On the synthesis of random fields from the spectrum. An application to the generation of hydrologic spatial processes, Water Resources Research, 10(4), 705-711, 1974.
- Shinozuka, M., Simulation of multivariate and multi-dimensional random processes, J. Acoust. Soc. Am., 49, 357-367, 1971.
- Vanmarcke, E., Random Fields: Analysis and Synthesis, The MIT Press, Cambridge, Mass., 1983.
- Wilson, J.W and E.A. Brandes, Radar measurement of rainfall -- a summary, Bulletin of the American Meteorological Society, 60(9), 1048-1058, 1979.

## APPENDIX A

### Turning Bands Method

Take a number  $L$  of lines of random direction intersecting at a certain point. For each line of direction  $\theta$ , generate a unidimensional process with zero mean and covariance  $C_{1,\theta}(\tau)$  at spatial lag  $\tau$ . Project each point, of coordinates  $(x,y)$ , for which one wants to generate a value of the two-dimensional random field, onto line  $i=1,2,\dots,L$ . Record the value  $Z_i(x,y)$  of the unidimensional process at the projection and repeat projection for all the other lines. The value  $Z(x,y)$  assigned to the point  $(x,y)$  is then:

$$Z(x,y) = \frac{1}{\sqrt{L}} \sum_{i=1}^L Z_i(x,y) \quad (\text{A-1})$$

Mantoglou and Wilson [1981] give the relationship of the unidimensional covariance  $C_{1,\theta}(\tau)$  to the two-dimensional one (in our case, characterized by  $\sigma^2$  and  $\rho(\tau_1,\tau_2)$ ). The generation of the unidimensional process on each line can be done using the spectral method of Shinozuka [1971]:

$$Z_i(\delta) = 2 \sum_{k=1}^M [S_{1,\theta}(\omega_k) \cdot \Delta\omega]^{1/2} \cdot \cos(\omega'_k \cdot \delta + \phi_k) \quad (\text{A-2})$$

where  $S_{1,\theta}(\cdot)$  is the spectral density function obtained as a Fourier transform of  $C_{1,\theta}(\tau)$ . Equation (A-2) assumes a discretization of the total spectrum  $\langle -\Omega, \Omega \rangle$  in  $M$  components of central frequencies  $\omega_k$ ;  $k=1,\dots,M$ , such that the difference  $\omega_k - \omega_{k-1}$  is independent of  $k$  and equal to  $\Delta\omega$ .  $\phi_k$  is a sequence of randomly distributed angles in  $\langle 0, 2\pi \rangle$ . The angle  $\omega'_k$  is the sum of the angle  $\omega_k$  and a small random angle distributed uniformly between  $\frac{-\Delta\omega'_k}{2}$  and  $\frac{\Delta\omega'_k}{2}$  with  $\Delta\omega'_k \leq \Delta\omega$ .

For the commonly used exponential anisotropic correlation function (Eq. (25)), Mantoglou and Wilson [1981] give:

$$S_{1,\theta}(\omega) = \frac{\sigma^2}{2} \cdot \frac{\omega}{h_1 h_2 [1 + \omega^2 (\frac{\cos^2 \theta}{h_1^2} + \frac{\sin^2 \theta}{h_2^2})]^{3/2}} \quad (\text{A-3})$$

where  $\theta$  is the angle of the turning bands line with the  $x$ -axis, and  $\sigma^2$  is the variance of the two-dimensional process.

In the special case of the isotropic correlation function (Eq. (26)), Mantoglou and Wilson [1981] give:

$$S_1(\omega) = \frac{\sigma^2}{2} \cdot \frac{\omega}{b^2 \left[1 + \frac{\omega^2}{b^2}\right]^{3/2}} \quad (\text{A-4})$$

where  $S_1(\omega)$  is the spectral density function along each line and  $\sigma^2$  is the variance of the two-dimensional process.